Nat Immunol. Author manuscript; available in PMC 2017 October 10.

Published in final edited form as:
Nat Immunol. 2017 June ; 18(6): 683–693. doi:10.1038/ni.3724.

Maintenance of the marginal zone B cell compartment specifically requires the RNA-binding protein ZFP36L1

Rebecca Newman[1,2], **Helena Ahlfors**[1], **Alexander Saveliev**[1], **Alison Galloway**[1], **Daniel J Hodson**[3], **Robert Williams**[1], **Gurdyal S. Besra**[4], **Charlotte N Cook**[5], **Adam F Cunningham**[5], **Sarah E Bell**[1], and **Martin Turner**[1,*]

[1]Laboratory of Lymphocyte Signalling and Development, The Babraham Institute, Babraham Research Campus, Cambridge, CB22 3AT, United Kingdom

[2]Immune Receptor Activation Laboratory, The Francis Crick Institute, 1 Midland Road, London, NW1 1AT, United Kingdom

[3]Department of Haematology, University of Cambridge, The Clifford Allbutt Building, Cambridge Biomedical Campus, Hills Road, Cambridge, CB2 0AH, United Kingdom

[4]School of Biosciences, University of Birmingham, Birmingham, B15 2TT, United Kingdom

[5]MRC Centre for Immune Regulation, School of Immunity and Infection, University of Birmingham, Birmingham, B15 2TT, United Kingdom

Abstract

RNA binding proteins (RBP) of the ZFP36 family are best known for inhibiting the expression of cytokines through binding to AU rich elements in the 3'UTR and promoting mRNA decay. Here we show an indispensible role for ZFP36L1 as the regulator of a post-transcriptional hub that determined the identity of marginal zone (MZ) B cells by promoting their proper localization and survival. ZFP36L1 controlled a gene expression program related to signaling, cell-adhesion and locomotion, in part by limiting the expression of the transcription factors KLF2 and IRF8, which are known to enforce the follicular B cell phenotype. These mechanisms emphasize the importance of integrating transcriptional and post-transcriptional processes by RBP for maintaining cellular identity between closely related cell types.

Marginal zone B (MZ B) cells surround the follicles of the spleen and are continuously exposed to blood-borne antigens. This positioning of MZ B cells enables them to provide

Contact Information martin.turner@babraham.ac.uk.

Author contributions

R.N. designed and did most experiments, H.A. Performed bioinformatics analysis, A.S. performed iCLIP analysis, A.G., S.E.B., D.J.H. and R.W. helped with mouse experiments, G.S.B provided NP-αGalCer, C.N.C. and A.F.C. performed some histology, R.N. and M.T. planned the project and wrote the manuscript.

Competing financial interests

The authors declare no competing financial interests.

Additional Title Page Footnotes

Role of Zfp36l1 in MZ B cells

Europe PMC Funders Author Manuscripts

immune surveillance, and shuttle antigen to follicular dendritic cells 1, 2. Their localization to the MZ and their trafficking to and from the B cell follicle also contributes to their survival 2, 3, 4, 5. Upon antigen encounter, MZ B cells are poised to promote T cell activation by presenting antigen as well as differentiating into plasmablasts6. Compared to follicular B (Fo B) cells, MZ B cells express greater amounts of surface IgM, CD35, CD21 and CD1d. Together with elevated expression of Toll-like receptors (TLR), these features facilitate rapid responses against blood-borne pathogens such as encapsulated bacteria7, 8.

MZ B cells develop through an intermediary population of marginal zone precursor (MZP) cells which express CD939. Selection of MZ B cells depends upon signaling by membrane immunoglobulin, Notch2 and the BAFF-R7 9. MZ- and Fo-B cells can be separated on the basis of their gene expression profiles10, and the differences in their transcriptomes contribute to the differential development, localization and function of these cells. Transcriptional regulators have been shown to have specific roles in MZ- and Fo-B cells. Notch2 is necessary to promote MZ B cell fate11, 12. The transcription factor IRF4 and its paralog IRF8 limit the size of MZ B cell pool13, and IRF4 regulates the positioning of cells in the MZ. The transcription factor KLF2 enforces the Fo B cell phenotype. In its absence, the MZ B cell pool is expanded14, 15. By contrast, KLF3, which may antagonise KLF2 promotes the development of MZ B cells16. These factors are frequently mutated in splenic MZ lymphoma17, suggesting they may also form part of a network that sustains the survival and localization of MZ B cells in pathological situations. Thus the interrelationship between transcriptional regulation, signal transduction and cell positioning for the development and survival of MZ B cells needs to be further understood17.

The post-transcriptional control of RNA regulated by RNA binding proteins (RBP) and non-coding RNAs complements transcriptional control by adding robustness to gene regulatory networks18. Deletion of Dicer19, or miRNA-14220, led to increased proportions of B cells with a MZ phenotype, suggesting that microRNAs suppress MZ B cell formation or survival. Retroviral expression of lin28b in haematopoietic stem cells promoted the development of MZ B cells21, 22, but roles for other RBP in MZ B cells have not been found.

The ZFP36 family of RBP are characterised by tandem CCCH-type zinc fingers, which bind RNA. By interacting with AU-rich elements (AREs) in the 3’UTR of mRNAs, these RBP promote RNA decay23. ZFP36 has been best characterised as a suppressor of cytokine production in innate immune cells; its relatives ZFP36L1 and ZFP36L2 play redundant roles during T and B lymphocyte development24, 25. The function of the ZFP36 family during the development and maintenance of mature B-lymphocytes has not been studied.

Here we demonstrate the indispensible role of ZFP36L1 in the maintenance of MZ B cells. Through analysis of the transcriptomes of primary mouse B cells, and the identification of ZFP36L1 targets in B cells by individual-nucleotide resolution cross-linking and immunoprecipitation (iCLIP), we identified the direct and indirect targets of ZFP36L1 in B cells, and determined a network of factors under the control of ZFP36L1 that promote MZ B cell localisation and survival. This study demonstrates that a single RBP can determine the cellular identity and ultimately survival of MZ B cells.

Results

MZ B cells specifically require ZFP36L1

To identify the roles of the ZFP36 family during lymphocyte development we first generated *Zfp36*$^{fl/fl}$hCD2-iCre^{+} (Supplementary Fig. 1), *Zfp36l1*$^{fl/fl}$hCD2-iCre^{+} and *Zfp36l2*$^{fl/fl}$hCD2-iCre^{+} mice in which each RBP was deleted early in lymphoid ontogeny. CD21^{hi}CD23^{-} MZ B cells were reduced nine-fold in *Zfp36l1*$^{fl/fl}$hCD2-iCre^{+} mice but were normal in *Zfp36*$^{fl/fl}$hCD2-iCre^{+} *and Zfp36l2*$^{fl/fl}$hCD2-iCre^{+} mice (Fig. 1a). CD21^{+}CD23^{+} Fo B cell numbers were slightly reduced in *Zfp36l1*$^{fl/fl}$hCD2-iCre^{+} mice (Fig. 1b). Transcripts encoding ZFP36, ZFP36L1 and ZFP36L2 family members were expressed in MZ B cells from C57BL/6 mice (Fig. 1c), indicating that the specific requirement for ZFP36L1 was not due to cell-specific mRNA expression. Thus, ZFP36L1 is required for the development or maintenance of MZ B cells, and its absence cannot be compensated for by ZFP36 or ZFP36L2.

B cell intrinsic requirement for ZFP36L1

When *Zfp36l1* was deleted at the pro-B cell stage, *Zfp36l1*$^{fl/fl}$mb1$^{cre/+}$ mice also showed a loss of MZ B cells compared to littermate *Zfp36l1*$^{fl/fl}$mb1$^{+/+}$ mice (data not shown). *Zfp36l1*$^{fl/fl}$CD23$^{cre/+}$ mice, in which *Zfp36l1* is deleted at the T2 B cell stage 26 also had a 10-fold reduction in the number of MZ B cells and a two-fold reduction in the number of CD93^{+}B220^{+}IgM^{high}CD21^{high} MZP B cells (Fig. 2a, b) compared to littermate *Zfp36l1*$^{fl/fl}$CD23$^{+/+}$ mice. We observed a small but significant 4-fold decrease in B220^{int}CD19^{+} B1 cells in the peritoneal cavity of *Zfp36l1*$^{fl/fl}$mb1$^{cre/+}$ mice compared to *Zfp36l1*$^{fl/fl}$mb1$^{+/+}$ mice with both CD5^{+} B1a cells and CD5^{-} B1b cells affected (Supplementary Fig. 2a-d). By contrast, B220^{+}CD19^{lo} B2 cell numbers in the peritoneal cavity were not different between *Zfp36l1*$^{fl/fl}$mb1$^{cre/+}$ and *Zfp36l1*$^{fl/fl}$mb1$^{+/+}$ mice (Supplementary Fig. 2a, b). Compared with the much larger effect of ZFP36L1 deletion on MZ B cell numbers, these observations suggested that there was only a minor role for ZFP36L1 in B1 B cells.

To further understand the role of ZFP36L1 in mature B cells we used CD23-Cre to express GFP-ZFP36L125. In *Rosa26*^{GFPZFP36L1}CD23$^{Cre/+}$ mice GFP-ZFP36L1 expression was observed from the T2 B cell stage (Supplementary Fig. 2e). MZ B cell numbers in *Rosa26*^{GFPZFP36L1}CD23$^{cre/+}$ mice are increased 1.5-fold compared to *Rosa26*^{GFPZFP36L1}CD23$^{+/+}$ mice, but there were no effects on Fo B cells or MZP B cells (Fig. 2c, d). Immunofluorescence staining of spleen sections with antibodies to identify MZ B cells indicated that the MZ was five-fold smaller in *Zfp36l1*$^{fl/fl}$CD23$^{cre/+}$ mice and expanded by 1.5 fold in *Rosa26*^{GFPZFP36L1}CD23$^{cre/+}$ mice compared to Cre-negative control mice (Fig. 2e, f). This demonstrates a requirement for ZFP36L1 from the T2 B cell stage for the development and/or maintenance of MZ B cells.

ZFP36L1 is required for the maintenance of MZ and MZP B cells

To test the continued requirement for ZFP36L1 in MZ B cells we used a Cre-ERT2 (oestrogen receptor fusion) transgene in which Cre activity is induced following tamoxifen administration to mice. In *Zfp36l1*$^{fl/fl}$ERT2$^{cre/+}$ mice seven days of tamoxifen treatment by

oral gavage induced the recombination and deletion of *Zfp36l1* in B cells, and a 1.3-fold decrease in MZ B cell numbers compared to *Zfp36l1*$^{+/+}$ERT2$^{cre/+}$ mice (Supplementary Fig. 3a, b). The recombination efficiency of *Zfp36l1* remained high at later time-points, and MZ B cells decreased 1.7-fold by day 10 and 3.2-fold by day 14 of tamoxifen treatment in *Zfp36l1*$^{fl/fl}$ERT2$^{cre/+}$ mice compared to *Zfp36l1*$^{+/+}$ERT2$^{cre/+}$ mice (Supplementary Fig. 3c-f). This on-going depletion of MZ B cells was selective, as Fo B cell numbers were not decreased at any of the three time-points tested (Supplementary Fig 3b, d, f). To exclude an effect of *Zfp36l1* deletion in non-haematopoietic cells in *Zfp36l1*$^{fl/fl}$ERT2$^{cre/+}$ mice27, 28, we reconstituted lethally irradiated CD45.1^{+} B6.SJL mice with bone marrow from CD45.2^{+} *Zfp36l1*$^{fl/fl}$ERT2$^{cre/+}$ or CD45.2^{+} *Zfp36l1*$^{+/+}$ERT2$^{cre/+}$ mice and eight weeks after reconstitution administered tamoxifen by oral gavage. Seven days following tamoxifen treatment the purified B cells from *Zfp36l1*$^{fl/fl}$ERT2$^{cre/+}$ showed more than 80% deletion of *Zfp36l1* (Fig. 3a). Chimeric mice reconstituted with *Zfp36l1*$^{fl/fl}$ERT2$^{cre/+}$ bone marrow had a selective loss of MZ and MZP B cells following seven days tamoxifen treatment (Fig. 3b), whilst Fo and transitional B cell subsets remained unchanged in number compared to the *Zfp36l1*$^{+/+}$ERT2$^{cre/+}$ chimeras (Fig. 3b; data not shown). Therefore *Zfp36l1* is dispensable for the maintenance of Fo B cells, but necessary for the persistence of MZ and MZP B cells.

To address whether ZFP36L1 affected B cell survival we used flow cytometry to measure the presence of active-caspase-3. There was a 2.5-fold increase in the proportion of MZ B cells positive for active-caspase-3^{+} in *Zfp36l1*$^{fl/fl}$ERT2$^{cre/+}$ compared to *Zfp36l1*$^{+/+}$ERT2$^{cre/+}$ chimaeras. In contrast, there was no increase in the proportion of active-caspase-3^{+} Fo B cells in *Zfp36l1*$^{fl/fl}$ERT2$^{cre/+}$ compared to *Zfp36l1*$^{+/+}$ERT2$^{cre/+}$ mice (Fig. 3c). Furthermore, the proportion of active-caspase 3+ cells was similarly increased amongst MZ but not Fo B cells from *Zfp36l1*$^{fl/fl}$mb1$^{cre/+}$ mice compared to *Zfp36l1*$^{fl/fl}$mb1$^{+/+}$ mice (Fig. 3d).

We assessed the turnover of MZ B cells in *Zfp36l1*$^{fl/fl}$mb1$^{cre/+}$ mice by measuring 2-bromodeoxyuridine (BrdU) labelling following administration for 14 days in the drinking water. BrdU is incorporated into highly proliferative pre-B cells in the bone marrow but not the non-proliferative transitional and naïve B cell subsets including MZ B cells29. At day 14 50% of MZ B cells were BrdU^{+} in *Zfp36l1*$^{fl/fl}$mb1$^{cre/+}$ mice, but only 30% of MZ B cells were BrdU^{+} in *Zfp36l1*$^{fl/fl}$mb1$^{+/+}$ mice (Fig. 3e). Approximately 17% of Fo B cells were BrdU+ in both *Zfp36l1*$^{fl/fl}$mb1$^{cre/+}$ mice and *Zfp36l1*$^{fl/fl}$mb1$^{+/+}$ mice. There was a small decrease of BrdU^{+} T2 and MZP B cells in *Zfp36l1*$^{fl/fl}$mb1$^{cre/+}$ mice compared to *Zfp36l1*$^{fl/fl}$mb1$^{+/+}$ mice (Supplementary Fig. 4a). By contrast, BrdU incorporation was reduced by 1.5-fold in MZ B cells and slightly increased in the T2 B cells of from in *Rosa26*^{GFPZFP36L1}CD23$^{cre/+}$ mice compared to *Rosa26*^{GFPZFP36L1}CD23$^{+/+}$ mice (Fig. 3f; Supplementary Fig. 4b). These data indicate that ZFP36L1 is not required for the survival of Fo B cells but is essential for the survival of MZ B cells.

Gene expression changes following inducible deletion of *Zfp36l1*

Zfp36l1 controls gene expression by promoting RNA decay23, 25. To identify direct targets of ZFP36L1 we performed RNA-seq on sorted MZ B cells from tamoxifen-treated *Zfp36l1*$^{fl/fl}$ERT2$^{cre/+}$ and *Zfp36l1*$^{+/+}$ERT2$^{cre/cre}$ mice. We observed a significant decrease in

the number of reads mapped within the floxed region of *Zfp36l1* in MZ B cells from *Zfp36l1*$^{fl/fl}$ERT2$^{cre/+}$ when compared to *Zfp36l1*$^{+/+}$ERT2$^{cre/cre}$ mice, (Supplementary Fig. 5a), indicating effective deletion of *Zfp36l1*. Upon loss of *Zfp36l1* we observed significant increases in the expression of 330 transcripts and diminished expression of 215 transcripts in *Zfp36l1*$^{fl/fl}$ERT2$^{cre/+}$ MZ B cells compared to *Zfp36l1*$^{+/+}$ERT2$^{cre/cre}$ MZ B cells. Of these, 84 and 26 transcripts were increased or decreased in expression by greater than 1.5 fold respectively (Fig. 4a, Supplementary Table 1). We also observed an increase in the expression of *Zfp36l2* upon deletion of *Zfp36l1* (Fig. 4a; Supplementary Fig. 5b), suggesting that ZFP36L2 cannot fully functionally compensate for ZFP36L1 in MZ B cells.

iCLIP can identify the direct targets and the specific nucleotide contacts between RBPs and RNAs, but this method has a requirement for large numbers of cells and is not sensitive enough to apply to the small numbers of MZ B cells available. Therefore, we used ZFP36L1 iCLIP data from activated Fo B cells25 to identify candidate mRNAs that can be bound by ZFP36L1. 73 genes showing increased expression in *Zfp36l1*$^{fl/fl}$ERT2$^{cre/+}$ compared to *Zfp36l1*$^{+/+}$ERT2$^{cre/cre}$ MZ B cells, 11 of which showed >1.5 fold change (Fig. 4b; Supplementary table 2, 3), were identified by iCLIP as possible direct targets of ZFP36L1. 24 transcripts with diminished expression in in *Zfp36l1*$^{fl/fl}$ERT2$^{cre/+}$ compared to *Zfp36l1*$^{+/+}$ERT2$^{cre/cre}$ MZ B cells also overlapped with the ZFP36L1 iCLIP data, however only one transcript, *Per2*, exhibited a fold change greater than 1.5 fold, suggesting that the iCLIP data is a stringent criterion for identifying direct targets of ZFP36L1 in MZ B cells.

To identify the functional roles of the genes that were differentially expressed between *Zfp36l1*$^{fl/fl}$ERT2$^{cre/+}$ and *Zfp36l1*$^{+/+}$ERT2$^{cre/cre}$ MZ B cells we performed a gene set enrichment analysis (GSEA) on all genes with significantly altered expression (padj<0.01) (Supplementary Table 2, 3). Because a number of the differentially expressed genes were recurrent within distinct GSEA pathways, to prevent overrepresentation of redundant GO terms, we summarised our GSEA analysis using a software tool to REduce and VIsualize Gene Ontology (REVIGO). This analysis indicated that there were a substantial number of differentially expressed transcripts involved in signaling; cellular adhesion and migration; cell cycle and proliferation; and programmed cell death (Fig. 4c). Transcripts that were expressed in reduced amounts did not comprise any common pathway or gene set, suggesting that these genes do not have a common functional role in MZ B cells.

The ZFP36 family of RBP was shown to promote cell quiescence25, 30. In *Zfp36l1*$^{fl/fl}$ERT2$^{cre/+}$ MZ B cells *Ccna2*, *E2f2*, *Cdc6*, *Pim1*, *Ccnd3* and *Cdk1* the mRNAs were ≥1.5 fold increased compared to *Zfp36l1*$^{+/+}$ERT2$^{cre/cre}$ MZ B cells (Supplementary Table 1, 2). To assess the consequences of this we analysed the proportion of MZ B cells in *Zfp36l1*-deficient mice expressing the cyclin-dependent kinase inhibitor p27^{KIP1} (*Cdkn1b*), a marker of cell quiescence. The expression of p27, and the proportion of p27^{+} MZ B cells isolated from tamoxifen-treated *Zfp36l1*$^{fl/fl}$ERT2$^{cre/+}$ mice was similar to those observed in *Zfp36l1*$^{+/+}$ERT2$^{cre/cre}$. P27 expression was unchanged in MZ B cells from *Zfp36l1*$^{fl/fl}$mb1$^{cre/+}$ mice compared to *Zfp36l1*$^{fl/fl}$mb1$^{+/+}$ mice (Supplementary Fig. 6a-c). Furthermore, the frequency of MZ B cells staining Ki67^{+} in *Zfp36l1*$^{fl/fl}$mb1$^{cre/+}$ mice was not different from MZ B cells of *Zfp36l1*$^{fl/fl}$mb1$^{+/+}$ mice, and the proportion of MZ- and Fo-B cells staining with the DNA binding dye DAPI as also unchanged in these mice.

(Supplementary Fig. 6d-g). Taken together, these data suggest that the reduction of MZ B cell numbers following developmentally programmed or induced deletion of *Zfp36l1* was not due to a loss of quiescence.

ZFP36L1 enforces MZ B cell identity

To further understand the changes in the MZ B cell transcriptome arising from deletion of *Zfp36l1* we compared transcripts that were differentially expressed between *Zfp36l1*$^{fl/fl}$ERT2$^{cre/+}$ and *Zfp36l1*$^{+/+}$ERT2$^{cre/cre}$ MZ B cells with transcripts that were differentially expressed between *Zfp36l1*$^{+/+}$ERT2$^{cre/cre}$ (wild-type) MZ and *Zfp36l1*$^{fl/fl}$ (wild-type) Fo B cells. 72% (54) of the transcripts with the greatest increase in expression in *Zfp36l1*$^{fl/fl}$ERT2$^{cre/+}$ compared to *Zfp36l1*$^{+/+}$ERT2$^{cre/cre}$ MZ B cells were more highly expressed in wild-type Fo B cells compared to wild-type MZ B cells (Fig. 5a and Supplementary table 4). Only a subset of the Fo B cell-enriched transcripts were increased in *Zfp36l1*$^{fl/fl}$ERT2$^{cre/+}$ MZ B cells (Fig. 5a), indicating that sorted *Zfp36l1*$^{fl/fl}$ERT2$^{cre/+}$ MZ B cells were not contaminated with *Zfp36l1*$^{fl/fl}$ERT2$^{cre/+}$ Fo B cells. Some transcripts that were more highly expressed in MZ B cells than in Fo B cells from wild-type mice, such as *PlexinD1* and *c-Myc*, were also increased in *Zfp36l1*$^{fl/fl}$ERT2$^{cre/+}$ compared to *Zfp36l1*$^{+/+}$ERT2$^{cre/cre}$ MZ B cells (Supplementary table 4). Thus, the remaining MZ B cells in *Zfp36l1*$^{fl/fl}$ERT2$^{cre/+}$ mice show increased expression of transcripts associated with a Fo B cell phenotype.

To determine the effect of GFP-ZFP36L1 on the transcriptome of Fo B cells, we used RNA-seq to compare the transcriptomes of sorted Fo B cells from *Rosa26*^{GFPZFP36L1}CD23$^{cre/+}$ mice to Fo B cells from *Rosa26*^{GFPZFP36L1}CD23$^{+/+}$ mice. Pairwise comparison with genes differentially expressed between wildtype Fo and MZ B cells indicated that Fo B cells from *Rosa26*^{GFPZFP36L1}CD23$^{cre/+}$ mice showed a trend towards increased expression of genes preferentially expressed in MZ B cells (Fig. 5b and Supplementary table 5) and reduced expression of genes characteristically expressed in Fo B cells (Fig. 5b and Supplementary table 5). A negative correlation was evident between genes differentially expressed in Fo B cells from *Rosa26*^{GFPZFP36L1}CD23$^{cre/+}$ mice and genes differentially expressed between *Zfp36l1*$^{fl/fl}$ERT2$^{cre/+}$ and ERT2$^{cre/cre}$ MZ B cells (Fig. 5c, Supplementary Table 6), suggesting that ZFP36L1 was required to maintain MZ B cell identity.

We next examined cell surface markers expressed by Fo B cells in *Rosa26*^{GFPZFP36L1}CD23$^{cre/+}$ mice. GFP^{+} Fo B cells from these mice showed increased expression of CD21, CD1d and MHCII compared to *Rosa26*^{GFPZFP36L1}CD23$^{+/+}$ mice (Fig. 5d), indicative of a phenotype and “activation” status that resembled MZ B cells. Furthermore, fluorescent antibody staining of spleen sections showed increased CD1d^{+} cells, which also expressed IgD, within the follicle of *Rosa26*^{GFPZFP36L1} CD23$^{cre/+}$ mice compared to *Rosa26*^{GFPZFP36L1}CD23$^{+/+}$ mice (Fig. 2f; Supplementary Fig. 7a **left panel, white arrowheads**).

MZ B cells show enhanced BCR-elicited calcium flux compared to Fo B cells31. Because a number of the transcripts differentially expressed between *Zfp36l1*$^{fl/fl}$ERT2$^{cre/+}$ and ERT2$^{cre/cre}$ MZ B cells had roles in cell signaling, we measured calcium flux elicited by surface IgM crosslinking.

As expected, BCR elicited calcium flux was enhanced in MZ B cells compared to Fo B cells in control *Zfp36l1*$^{fl/fl}$mb1$^{+/+}$ mice (Fig. 5e, f), while calcium flux in MZ B cells from *Zfp36l1*$^{fl/fl}$mb1$^{cre/+}$ was similar to that observed in Fo B cells (Fig. 5e). Calcium flux elicited by BCR crosslinking in CD93^{+} transitional B cell subsets (data not shown) or CD21^{+}CD23^{+} Fo B cells from *Zfp36l1*$^{fl/fl}$mb1$^{cre/+}$ mice was not different from that elicited in the same subsets from *Zfp36l1*$^{fl/fl}$mb1$^{+/+}$ mice (Fig. 5e).

Incubation of cells with EGTA chelates extracellular calcium and limits BCR stimulated calcium flux to that released from internal stores. Stimulation with anti-IgM elicited less calcium release in EGTA-treated MZ B cells from *Zfp36l1*$^{fl/fl}$mb1$^{cre/+}$ mice than from *Zfp36l1*$^{fl/fl}$mb1$^{+/+}$ mice (Fig. 5e). This indicates the defective release of calcium from the internal stores of *Zfp36l1*$^{fl/fl}$mb1$^{cre/+}$ MZ B cells. Thus, ZFP36L1 enhances BCR signaling in MZ B cells.

To investigate the function of the residual MZ B cells in the ZFP36L1-deficient mice, we immunized *Zfp36l1*$^{fl/fl}$CD23$^{cre/+}$, *Rosa26*^{GFPZFP36L1} CD23$^{cre/+}$ and CD23$^{+/+}$ littermate control mice with the CD1d-restricted antigen NP-α-GalCer32. Four days post-immunization the titer of NP-specific IgM in serum was similar in *Zfp36l1*$^{fl/fl}$CD23$^{cre/+}$ and *Zfp36l1*$^{fl/fl}$CD23$^{+/+}$ mice (Supplementary Fig. 7b), indicating that MZ B cell numbers ZFP36L1-deficient mice were not limiting the antibody response to antigen *in vivo*. This data suggests that ZFP36L1 does not play a role in the MZ B cell response to CD1d-restricted humoral responses *in vivo*, but enforces the MZ B cell phenotype in mice.

ZFP36L1 targets transcription factors important for MZ B cell identity

Loss of IRF8 leads to an enlarged MZ B cell compartment13, suggesting a role for IRF8 in limiting MZ B cell numbers. *Irf8* mRNA was increased 1.3-fold in MZ B cells from *Zfp36l1*$^{fl/fl}$ERT2$^{cre/+}$ compared to *Zfp36l1*$^{+/+}$ERT2$^{cre/cre}$ MZ B cells (Fig. 6a), and was decreased in in Fo B cells from *Rosa26*^{GFPZFP36L1}CD23$^{cre/+}$ mice compared to Fo B cells from *Rosa26*^{GFPZFP36L1}CD23$^{+/+}$ mice (Fig. 6b). IRF8 protein expression was also elevated in MZ B cells from *Zfp36l1*$^{fl/fl}$mb1$^{cre/+}$ compared to *Zfp36l1*$^{fl/fl}$mb1$^{+/+}$ mice (Fig. 6c, d). *Irf8* mRNA contains a highly conserved ARE in its 3'UTR and was bound by ZFP36L1 in the iCLIP performed on activated B cells (Fig. 6e), indicating it is a likely direct target of ZFP36L1 in MZ B cells.

To assess whether IRF8 target genes are likely to contribute to the loss of MZ B cells in the absence of Zfp36l1 we asked if transcripts that were differentially expressed between *Zfp36l1*$^{fl/fl}$ERT2$^{cre/+}$ and *Zfp36l1*$^{fl/fl}$ERT2$^{+/+}$ MZ B cells were identified as IRF8 targets in high-quality ChIP-seq data33. We found that a subset of the genes that were enriched in WT Fo B cells compared to wildtype MZ B cells and had increased expression in *Zfp36l1*$^{fl/fl}$ERT2$^{cre/+}$ compared to *Zfp36l1*$^{+/+}$ERT2$^{cre/cre}$ MZ B cells were bound by IRF8 (Fig. 6f). This suggests that increased expression of IRF8 contributes directly to the altered expression of these genes in the absence of ZFP36L1. Furthermore, the distribution of direct ZFP36L1 targets identified by iCLIP cells showed minimal overlap with IRF8 target genes (Fig. 6f, g). This indicates that ZFP36L1 and IRF8 generally act in a hierarchical manner, whereby ZFP36L1 targets a range of genes including IRF8, which in turn targets genes important for cell survival, localisation, signaling and maintenance of MZ B cell identity.

Klf2 mRNA was increased 3.1 fold (Fig. 7a) and KLF2 protein was also increased as assessed by flow cytometry (Fig. 7b, c) when *Zfp36l1*$^{fl/fl}$ERT2$^{cre/+}$ and *Zfp36l1*$^{+/+}$ERT2$^{cre/cre}$ MZ B cells were compared. *Klf2* mRNA contains a TATTTATT ARE in its 3'UTR, which is conserved amongst mammalian species that have a *Klf2* ortholog (Fig. 7d). iCLIP analysis indicated that ZFP36L1 binds in this ARE (Fig. 7d); however the data did not reach statistical significance due to low KLF2 mRNA abundance in activated B cells15, 34. Thus, ZFP36L1 may directly limit expression of KLF2.

To understand if KLF2 contributed to the altered gene expression profile of *Zfp36l1*$^{fl/fl}$ERT2$^{cre/+}$ MZ B cells we used KLF2 ChIP-seq data35 and microarray analysis of transcripts differentially expressed between Klf2$^{fl/fl}$-CD19Cre and wildtype B cells14 to generate a list of candidate KLF2 target genes relevant to B cells. This list identified a set of genes that were bound by KLF2, increased in *Zfp36l1*$^{fl/fl}$ERT2$^{cre/+}$ compared to *Zfp36l1*$^{+/+}$ERT2$^{cre/cre}$ MZ B cells, and increased in wild-type Fo B cells than in wild-type MZ B cells (Fig. 7e). Furthermore, this analysis showed that among the transcripts increased in *Zfp36l1*$^{fl/fl}$ERT2$^{cre/+}$ MZ B cells, the KLF2-bound genes were generally absent from both the ZFP36L1 iCLIP dataset and the IRF8 ChIPseq dataset (Fig. 7f), indicating that KLF2 overexpression in *Zfp36l1*$^{fl/fl}$ERT2$^{cre/+}$ MZ B cells was consequential for the transcriptome. Taken together, these analyses suggest a model whereby ZFP36L1 limits the expression of a number of genes including the transcription factors IRF8 and KLF2, which in turn regulate genes important for MZ B cell identity and survival (Supplementary Fig. 7c).

ZFP36L1 regulates the localization of B cells

GSEA on 116 transcripts that were both increased in *Zfp36l1*$^{fl/fl}$ERT2$^{cre/+}$ MZ B cells and decreased in Fo B cells from *Rosa26*^{GFPZFP36L1} CD23$^{cre/+}$ mice (Supplementary Fig. 8a) identified pathways involved in B cell trafficking (Supplementary Fig. 8b).

Flow cytometry analysis indicated increased expression of CD62L and β_7 integrin but no difference in CD69, a surrogate marker for S1Pr1 expression, on the cell surface of *Zfp36l1*$^{fl/fl}$mb1$^{cre/+}$ MZ B cells compared to *Zfp36l1*$^{fl/fl}$mb1$^{+/+}$ controls and decreased expression of CD62L and β_7 integrin on Fo B cells from *Rosa26*^{GFPZFP36L1}CD23$^{cre/+}$ mice compared to *Rosa26*^{GFPZFP36L1}CD23$^{+/+}$ mice (Fig. 8a). We observed little, if any, difference in the surface expression of CXCR4, CXCR5, β_1 integrin and LFA-1 on the surface of MZ and Fo B cells from *Zfp36l1*$^{fl/fl}$mb1$^{cre/+}$ mice compared to *Zfp36l1*$^{fl/fl}$mb1$^{+/+}$ mice (data not shown). S1Pr1 mRNA was also not different in MZ B cells from *Zfp36l1*$^{fl/fl}$ERT2$^{cre/+}$ compared to *Zfp36l1*$^{+/+}$ERT2$^{cre/cre}$ MZ B cells (Supplementary Fig. 8c). To assess whether ZFP36L1 affected the localisation of MZ B cells we measured by flow cytometry the binding of phycoerthrin-conjugated antibody to CD19 (CD19-PE) on MZ B cells following intravenous administration to mice. The binding of CD19-PE to MZ B cells from *Zfp36l1*$^{fl/fl}$CD23$^{cre/+}$ mice was reduced by 1.5-fold compared to its binding to MZ B cells from *Zfp36l1*$^{fl/fl}$CD23$^{+/+}$ mice (Fig. 8b), indicating that ZFP36L1 promoted localisation to the MZ.

We generated mixed bone marrow chimaeras by reconstituting lethally irradiated B6.SJL mice with bone marrow from *Zfp36l1*$^{fl/fl}$ERT2$^{cre/+}$ or *Zfp36l1*$^{+/+}$ERT2$^{cre/+}$ mice together with bone marrow from μMT mice. Following reconstitution we administered tamoxifen to

induce deletion of *Zfp36l1* and measured the localisation of CD1d+ cells by antibody staining of splenic tissue sections. We observed an increased proportion of CD1d^{+} B cells within the splenic follicles of *Zfp36l1*$^{fl/fl}$ERT2$^{cre/+}$:μMT compared to *Zfp36l1*$^{+/+}$ERT2$^{cre/+}$:μMT chimaeras (Fig. 8c). CD1d^{+} B cells within the splenic follicles of *Zfp36l1*$^{fl/fl}$ERT2$^{cre/+}$:μMT chimaeras did not express IgD indicating they were MZ B cells (Supplementary Fig. 7a **right panel, white arrowheads**). We defined the boundaries of the splenic follicle using MOMA-1 staining (Supplementary Fig. 8e) and quantified the MFI of CD1d within the follicle. CD1d MFI was increased in the splenic follicle of *Zfp36l1*$^{fl/fl}$ERT2$^{cre/+}$:μMT compared to *Zfp36l1*$^{+/+}$ERT2$^{cre/+}$:μMT chimaeras (Fig. 8d).

The MFI of CD1d within the MZ of *Zfp36l1*$^{fl/fl}$ERT2$^{cre/+}$:μMT chimaeras mice was not increased (Fig. 8d) indicating that the increased CD1d MFI within the follicle of *Zfp36l1*$^{fl/fl}$ERT2$^{cre/+}$:μMT did not result from an increase of CD1d expression on all B cells. By normalising the MFI of CD1d within the splenic follicle to the MFI of CD1d within the Fo and MZ, confirmed this result (Fig. 8d). Thus, ZFP36L1 is required for the proper localization of MZ B cells.

Discussion

Here we report an essential role for ZFP36L1 in the maintenance of MZ B cells. ZFP36L1 mediates this role by interacting with, and limiting the expression of, a set of transcripts that promote the Fo B cell phenotype. The relevant targets of ZFP36L1 in this context were distinct from previously identified ZFP36L1 targets and included the transcription factors IRF8 and KLF2 and regulators of adhesion and migration.

This ability of ZFP36L1 to regulate different transcripts at discrete stages of development is reminiscent of transcription factors controlling gene expression characteristic of a particular developmental stage36. Regulation by ZFP36L1 can be considered to be a post-transcriptional RNA operon or “regulon”37 maintaining the identity of MZ B cells. ZFP36L1 related proteins regulate cell fate in other developmental biology systems. In *Caenorhabditis elegans,* the germline and somatic cell fates are regulated by multiple RBPs, many of which contain tandem CCCH zinc fingers. Amongst these, OMA-138 and POS-139 bind with high affinity to AU-rich sequences in 3’UTRs of mRNAs. Systems analysis indicates extensive crosstalk between RBP and transcription factors in *C. elegans*40. Our findings indicate the existence of similar networks in mammalian cells. Establishing this principle in additional mammalian systems will require both the identification of the relevant RBP and the bound targets.

The specific requirement for *Zfp36l1* in MZ B cells contrasts with the redundant function of *Zfp36l1* and *Zfp36l2* in early lymphocyte development25. ZFP36L1 binds to *Zfp36l2* mRNA and the abundance of *Zfp36l2* mRNA was increased in *Zfp36l1*$^{+/+}$ERT2$^{cre/+}$ MZ B cells suggesting ZFP36L1 suppresses its paralog in MZ B cells. It thus appears that *Zfp36l2* could not compensate for the absence of ZFP36L1 in MZ B cells. This may reflect differences in the post-translational biology of the encoded RBPs, such as the effects of specific phosphorylation or of multi-protein complex formation. Alternatively, there may be differences between ZFP36 family members in their ability to bind to and regulate specific

Europe PMC Funders Author Manuscripts

targets. Extensive further work is required to understand the molecular basis for the redundant and non-redundant functions of these RBPs.

We identified IRF8 and KLF2 as direct targets of ZFP36L1 that regulate a number of genes important for MZ B cell identity. The molecular basis for KLF2 regulation of the MZ B cell pool may also relate to its ability to control expression of adhesion receptors, while the mechanisms by which IRF8 limits the size of the MZ B cell compartment is unclear 13 41. Many, but not all, of the indirect changes in the transcriptome of *Zfp36l1*$^{+/+}$ERT2$^{cre/cre}$ MZ B cells appeared to stem from the increased expression of IRF8 or KLF2, as these transcription factors account for 18/54 differentially expressed Fo B cell “signature” genes. Many KLF2 targets, that were not ZFP36L1 targets, were increased in *Zfp36l1*$^{+/+}$ERT2$^{cre/cre}$ MZ B cells and a number of these were also suppressed in Fo B cells from *Rosa26*^{GFPZFP36L1}CD23$^{cre/+}$ mice. Thus the transcriptome of MZ B cells is regulated by network of factors, acting transcriptionally and post-transcriptionally, in which ZFP36L1 is a major hub. Additional ZFP36L1 targets identified in the iCLIP and increased in *Zfp36l1*$^{+/+}$ERT2$^{cre/+}$ MZ B cells may contribute to the abnormal localisation and survival of MZ B cells. Pim1 kinase42, 43; KIAA0101 (2810417H13Rik)44; Myadm (myeloid-associated differentiation marker) a putative adapter protein of uncertain function45, 46; Txnrd1 (thioredoxin reductase 1) an enzyme that catalyzes the reduction of thioredoxin47, 48; and Bhlhe4049; have all been implicated in adhesion and metastasis. ZFP36L1 may act to promote the interaction between MZ B cells and the unique extracellular matrix components that are enriched in the MZ and play an important role in promoting the survival of MZ B cells3. These mechanisms protect MZ B cells from apoptosis. It is therefore tempting to speculate that ZFP36L1-deficient MZ B cells are lacking these pro-survival signals when access to the MZ is limited. This may be analogous to the process of anoikis, whereby detachment of adherent cells from a niche can lead to programmed cell death50.

In summary, our data suggest that ZFP36L1 acts post-transcriptionally to enforce the phenotype of MZ B cells and in its absence MZ B cells are mislocalized and die. It will be important for future studies to establish whether these mechanisms contribute to pathology in lymphoma or autoimmune disease.

Methods

Reagents, antibodies and oligonucleotides

This information is provided in Supplementary Tables 7 (reagents), 8 (antibodies) and 9 (oligonucleotides).

Mouse strains and animal procedures

Mice on the C57BL/6 background used in this study were derivatives of the following: Tg(CD2-cre)4Kio51, CD79a$^{tm1(cre)Reth}$52, Tg(Fcer2a-cre)5Mbu26, Gt(ROSA)26Sor$^{tm1(cre/ERT2)Thl}$ 53, Zfp36^{tm1Tnr} (Supplementary Fig. 1), Zfp36l1$^{tm1.1Tnr}$24, Zfp36l2$^{tm1.1Tnr}$24, Gt(Rosa)26Sor$^{tm1(GFPZfp36l1)Tnr}$ 25, B6.129S1-*Bcl2l11*$^{tm1.1Ast}$/J54. All mice were aged between 8-12 weeks. B6.SJL mice, which were used in competitive bone marrow chimera experiments, are Ly5.1 (CD45.1 allotype) C57BL/6 congenic mice

obtained from Jackson labs, USA. For bone marrow chimeras, B6.SJL recipient mice were irradiated and reconstituted with a total of $3x10^6$ donor bone marrow cells by i.v. injection. Reconstituted mice were fed neomycin sulphate (Sigma) in their drinking water for four weeks post-reconstitution, and were analysed after 8-10 weeks. In the case of μMT chimeras, of the $3x10^6$ donor BM cells, 80% were taken from μMT mice, and 20% from either *Zfp36l1*$^{fl/fl}$ERT2$^{cre/+}$ or ERT2$^{cre/+}$controls. BrdU (Sigma) was administered at 0.8mg/ml in drinking water. Unless otherwise stated, control mice used in experiments were littermate controls that were negative for Cre. Tamoxifen (Cambridge Bioscience Ltd.) was prepared in sunflower oil containing 10% ethanol to a final concentration of 50mg/ml. Daily dosage for mice was 200mg/kg. Tamoxifen was fed to mice for two consecutive days using a bulb-tipped reusable feeding needle. After induction of cre, mice were returned to stock and euthanized at the appropriate time point. 0.8μg of PE-labelled anti-mouse CD19 antibody in PBS was administered intravenously and mice were culled at 5 minutes following injection. Spleen cell suspensions were prepared and surface stained as described. The Animal Welfare and Experimentation Committee of Babraham Institute and the UK Home Office approved all animal procedures at the Babraham Institute.

Immunizations and ELISAs

Mice were immunized i.v. with 1μg/ml NP-αGalCer32 in 200μl PBS containing 0.05% BSA that had been sonicated. Serum was prepared from blood collected at day 4 post-immunization. Relative endpoint titres for serum antibody were determined by ELISA. For determination of NP-specific antibodies, ELISA plates (Nunc Maxisorp) were coated with NP(23)-BSA (BSA, Biosearch Technologies) and blocked with 1% BSA in PBS. Serial dilutions of serum samples (0.1% BSA/PBS) were added and incubated overnight. Bound IgM-specific antibodies were detected with biotinylated anti-mouse IgM-specific Ig (Southern Biotech) followed by streptavidin HRP (Southern Biotech) and developed with Sigma Fast O-phenylenediamine dihydrochloride (Sigma-Aldrich) as a substrate and the absorbance at 490nm determined. Absorbance values were plotted from serially diluted samples and values, which fell into the linear range of the curve were used to calculate endpoint titres.

Flow cytometry

B cell populations were analysed using antibodies against B220, CD19, CD21, CD23, CD93, IgD and IgM (Supplementary table 8). B cells analysed in the bone marrow were as follows: Immature B cells, B220$^+$IgM$^+$IgD$^-$; Recirculating B cells, B220$^+$IgM$^-$IgD$^+$. B cells analysed in the spleen were as follows: T1 B cells, B220$^+$CD93$^+$CD23$^-$IgM^{hi}; T2 B cells, B220$^+$CD93$^+$CD23$^+$IgM^{hi}; T3 B cells, B220$^+$CD93$^+$CD23$^+$IgM$^+$; marginal zone precursors, B220$^+$CD93$^+$CD21^{hi}IgM^{hi}; marginal zone B cells, B220$^+$CD93$^-$CD21^{hi}CD23$^-$ or B220$^+$CD9$^+$CD1d^{hi} and follicular B cells, B220$^+$CD93$^-$CD21$^+$CD23$^+$. B cells analysed in the peritoneal cavity were as follows: B1 B cells, B220^{lo}CD19$^+$, B2 B cells; B220$^+$CD19^{lo}; B1a cells, B220^{lo}CD19$^+$CD5$^+$IgM$^+$; B1b cells, B220^{lo}CD19$^+$CD5$^-$IgM$^+$. Fixable viability dye eFluor780 was used to assess cell viability. BrdU was detected using the BrdU flow kit (BD), following the manufacturer's instructions. Cells were analysed using a BD LSRFortessa flow cytometer. To measure apoptosis, $5x10^6$ cells were stained intracellularly

Europe PMC Funders Author Manuscripts

with a FITC conjugated rabbit monoclonal antibody, which recognises active Caspase-3 (BD Biosciences).

Calcium flux analysis

Splenocytes were loaded for 30min at 37°C in the dark with 0.6μM Ca^{2+} indicator PBX (BD) in serum free DMEM (5-10x10^6 cells). Cells were then stained with surface antibodies at RT, and resuspended in serum free Hanks medium. Cells were pre-treated with 10mM EGTA for 1 minute if required, before being stimulated with 10μg/ml goat polyclonal α-IgM F'ab fragment (Jackson ImmunoResearch). Fluorescence emission (525nm) was measured using a 488nm laser and 530/30 filter on a BD LSRFortessa flow cytometer.

B cell purification and sorting

B cells from spleen or peripheral lymph nodes were isolated with a B cell Isolation Kit from Miltenyi Biotech. To purify specific B cell subsets, cells were subsequently sorted using a BD FACSAria III or a BD FACSAria Fusion, using staining described above.

DNA isolation, RNA extraction and RT-qPCR assays

Total RNA was extracted from purified B cells using TRIzol (LifeTech) or RNeasy Micro or Mini Kit (Qiagen). RNA was treated with DNase I before reverse transcription into cDNA. ZFP36 family expression was analysed using custom and commercially available TaqMan assays with specific primers (Supplementary Table 9). Expression of mRNA was calculated using a standard curve and normalised to the expression of β2M. Genomic DNA was extracted from purified B cells using Cell lysis solution (Qiagen) containing proteinase K (Roche). Protein was removed by salt precipitation, and the DNA was isolated using isopropanol. Relative abundance of ZFP36l1 exon 2 was analysed by quantitative PCR with specific primers (Supplementary Table 9), qPCR assays were performed with Platinum SYBR Green qPCR SuperMix (Life Technologies). Relative abundance of ZFP36l1 was calculated using the comparative threshold cycle (ΔΔCT) method and results were normalised to the expression of TBP.

Immunofluorescence

Spleens were frozen in OCT compound on dry-ice, and sectioned on the cryostat (7-10μm thick). Sections were air dried overnight, then fixed in ice cold acetone for 15 mins at 4°C. Tissue sections were rehydrated in PBS for 10, and blocked in 5% NRS. Sections were stained in 5% NRS at 4°C overnight in a humidified chamber to detect IgM and MOMA-1, or CD1d, IgD and MOMA-1. Slides were washed PBS, and mounted in ProLong Gold antifade reagent (Thermo Fischer). Images were acquired at x10 or ×20 magnification using a DeltaVision widefield fluorescence microscope (GE Healthcare). Images were quantified using Image-J software (NIH). MZ width was measured using Image-J software. At least 10 follicles per genotype were imaged, measurements were taken from the edge of MOMA-1^+ cells to the edge of $CD1d^+$ staining. A number of measurements were taken per follicle to account for variability. CD1d MFI (-background) was calculated using Image-J (NIH). Follicular area was defined using MOMA-1 (CD169) staining. MFI was then calculated for this area (see Supplementary Fig. 8e). MZ area was defined as $CD1d^+$ area outside

MOMA-1 and IgD staining (see Supplementary Fig. 8e). Background fluorescence was calculated and subtracted from MFI values for MZ and FO. Measurements were taken from 10 follicles from 2 $ERT2^{cre/+}$ chimeras, and 25 follicles from 2 *Zfp36l1*$^{fl/fl}$$ERT2^{cre/+}$ chimeras.

Library preparation and high-throughput sequencing

Sorted MZ or FO B cells from individual control mice were independently processed for RNA extraction. RNAseq libraries were obtained using a TruSeq Stranded mRNA Sample Prep Kit (Illumina) or SMARTer Ultra Low Input RNA v4 and SMARTer Low Input Library Prep Kit V2 (Clontech). Low input libraries were prepared and sequenced from total RNA at Aros Applied Biotechnology A/S. RNAseq libraries were sequenced using the HTSeq2000 (Illumina). 100bp single end or paired end sequencing was performed on all libraries.

Bioinformatics for RNAseq

Quality of sequencing data was analysed using FastQC (http://www.bioinformatics.babraham.ac.uk/projects/fastqc/). Reads were mapped to mouse genome (GRCm38) using Tophat255. Reads aligning to genes were counted using htseq-count56 and analysis of differentially expressed genes was performed using the DESeq2 (R/bioconductor package)57. Reads were visualised using Integrative Genomics Viewer (IGV)58, 59. Gene set enrichment analysis was performed using ToppGene60 and the enriched GO biological processes were visualised using Revigo61. iCLIP data was analysed as previously described25.

To analyse conservation of Zfp36l1 binding motif in its target genes, the 3'UTR sequence of selected gene in mouse was queried against synthenic sequences in eutherian mammals using Ensembl Perl API.

Bioinformatics for publically available data

ChIP-seq data for Klf235 and IRF833 and Affymetrix data for *Klf2*-deficient FO B cells14 were downloaded from the Gene Expression Omnibus. The Affymetrix data was analysed using R/Bioconductor package affy62. Reads from ChIP-seq data were mapped to mouse genome (GRCm38) using Bowtie263 and peaks were called using MACS264. Only reproducible peaks were considered. Peaks were visualised using IGV.

Statistical analysis

Mann-Whitney tests were performed for statistical analysis of non-sequencing data. Additional details regarding sample size and statistics used have been provided in the figure legends where relevant.

Data availability

The RNA-seq data are available in the Gene Expression Omnibus (GEO) database (http://www.ncbi.nlm.nih.gov/gds) under the accession numbers: GSE79632 (Transcriptome of Zfp36l1-deficient MZ B cells, WT MZ B cells and WT FO B cells), GSE79632 (Transcriptome of GFP-ZFP36L1 expressing and WT FO B cells). ChIP-seq data for Klf235 and IRF833 and Affymetrix data for *Klf2*-deficient FO B cells14 were downloaded from the

Gene Expression Omnibus. The data the support the findings of this study are available from the corresponding author upon request.

Supplementary Material

Refer to Web version on PubMed Central for supplementary material.

Acknowledgments

We thank M. Busslinger for the CD23-Cre expressing mice, M. Reth for the mb1-Cre expressing mice, T. Ludwig for the ERT2-cre expressing mice and D. Kioussis for the hCD2-iCre-expressing mice. This work was funded by a GSK-CASE studentship to RN and funding from the Biotechnology and Biological Sciences Research Council, The Medical Research Council and Bloodwise. We thank K. Bates, R. Walker, A.Davies and L. Waugh and members of the Biological Services Unit for technical support; D. Bell and P. Tolar for help with immunofluorescence analysis; members of the laboratory, L. Webb, M. Linterman and T. Arnon for helpful advice.

References

1. Cinamon G, Zachariah MA, Lam OM, Foss FW Jr, Cyster JG. Follicular shuttling of marginal zone B cells facilitates antigen transport. Nature immunology. 2008; 9:54–62. [PubMed: 18037889]
2. Arnon TI, Horton RM, Grigorova IL, Cyster JG. Visualization of splenic marginal zone B-cell shuttling and follicular B-cell egress. Nature. 2013; 493:684–688. [PubMed: 23263181]
3. Song J, et al. Extracellular matrix of secondary lymphoid organs impacts on B-cell fate and survival. Proceedings of the National Academy of Sciences of the United States of America. 2013; 110:E2915–E2924. [PubMed: 23847204]
4. Simonetti G, et al. IRF4 controls the positioning of mature B cells in the lymphoid microenvironments by regulating NOTCH2 expression and activity. J Exp Med. 2013; 210:2887–2902. [PubMed: 24323359]
5. Fasnacht N, et al. Specific fibroblastic niches in secondary lymphoid organs orchestrate distinct Notch-regulated immune responses. J Exp Med. 2014; 211:2265–2279. [PubMed: 25311507]
6. Cerutti A, Cols M, Puga I. Marginal zone B cells: virtues of innate-like antibody-producing lymphocytes. Nature reviews. Immunology. 2013; 13:118–132.
7. Pillai S, Cariappa A. The follicular versus marginal zone B lymphocyte cell fate decision. Nature reviews. Immunology. 2009; 9:767–777.
8. Martin F, Kearney JF. Marginal-zone B cells. Nature reviews. Immunology. 2002; 2:323–335.
9. Srivastava B, Quinn WJ, Hazard K, Erikson J, Allman D. Characterization of marginal zone B cell precursors. J Exp Med. 2005; 202:1225–1234. [PubMed: 16260487]
10. Kleiman E, et al. Distinct Transcriptomic Features are Associated with Transitional and Mature B-Cell Populations in the Mouse Spleen. Frontiers in immunology. 2015; 6:30. [PubMed: 25717326]
11. Tan JB, et al. Lunatic and manic fringe cooperatively enhance marginal zone B cell precursor competition for delta-like 1 in splenic endothelial niches. Immunity. 2009; 30:254–263. [PubMed: 19217325]
12. Witt CM, Won WJ, Hurez V, Klug CA. Notch2 haploinsufficiency results in diminished B1 B cells and a severe reduction in marginal zone B cells. J Immunol. 2003; 171:2783–2788. [PubMed: 12960298]
13. Feng J, et al. IFN regulatory factor 8 restricts the size of the marginal zone and follicular B cell pools. J Immunol. 2011; 186:1458–1466. [PubMed: 21178004]
14. Hart GT, Wang X, Hogquist KA, Jameson SC. Krüppel-like factor 2 (KLF2) regulates B-cell reactivity, subset differentiation, and trafficking molecule expression. PNAS. 2010; 2:1–6.
15. Winkelmann R, et al. B cell homeostasis and plasma cell homing controlled by Kruppel-like factor 2. Proceedings of the National Academy of Sciences of the United States of America. 2011; 108:710–715. [PubMed: 21187409]
16. Vu TT, et al. Impaired B Cell Development in the Absence of Kruppel-like Factor 3. Journal of immunology. 2011; 187:5032–5042.

17. Clipson A, et al. KLF2 mutation is the most frequent somatic change in splenic marginal zone lymphoma and identifies a subset with distinct genotype. Leukemia. 2015; 29:1177–1185. [PubMed: 25428260]
18. Turner M, Galloway A, Vigorito E. Noncoding RNA and its associated proteins as regulatory elements of the immune system. Nature immunology. 2014; 15:484–491. [PubMed: 24840979]
19. Belver L, de Yebenes VG, Ramiro AR. MicroRNAs prevent the generation of autoreactive antibodies. Immunity. 2010; 33:713–722. [PubMed: 21093320]
20. Kramer NJ, et al. Altered lymphopoiesis and immunodeficiency in miR-142 null mice. Blood. 2015; 125:3720–3730. [PubMed: 25931583]
21. Yuan J, Nguyen CK, Liu X, Kanellopoulou C, Muljo SA. Lin28b reprograms adult bone marrow hematopoietic progenitors to mediate fetal-like lymphopoiesis. Science. 2012; 335:1195–1200. [PubMed: 22345399]
22. Zhou Y, et al. Lin28b promotes fetal B lymphopoiesis through the transcription factor Arid3a. J Exp Med. 2015; 212:569–580. [PubMed: 25753579]
23. Brooks, Sa, Blackshear, PJ. Tristetraprolin (TTP): Interactions with mRNA and proteins, and current thoughts on mechanisms of action. Biochim Biophys Acta. 2013; 1829:666–679. [PubMed: 23428348]
24. Hodson DJ, et al. Deletion of the RNA-binding proteins ZFP36L1 and ZFP36L2 leads to perturbed thymic development and T lymphoblastic leukemia. Nature immunology. 2010; 11:717–724. [PubMed: 20622884]
25. Galloway A, et al. RNA-binding proteins ZFP36L1 and ZFP36L2 promote cell quiescence. Science. 2016; 352:453–459. [PubMed: 27102483]
26. Kwon K, et al. Instructive role of the transcription factor E2A in early B lymphopoiesis and germinal center B cell development. Immunity. 2008; 28:751–762. [PubMed: 18538592]
27. Bell SE, et al. The RNA binding protein Zfp36l1 is required for normal vascularisation and post-transcriptionally regulates VEGF expression. Developmental dynamics : an official publication of the American Association of Anatomists. 2006; 235:3144–3155. [PubMed: 17013884]
28. Stumpo DJ, et al. Chorioallantoic fusion defects and embryonic lethality resulting from disruption of Zfp36L1, a gene encoding a CCCH tandem zinc finger protein of the Tristetraprolin family. Mol Cell Biol. 2004; 24:6445–6455. [PubMed: 15226444]
29. Allman D, et al. Resolution of three nonproliferative immature splenic B cell subsets reveals multiple selection points during peripheral B cell maturation. J Immunol. 2001; 167:6834–6840. [PubMed: 11739500]
30. Vogel KU, Bell LS, Galloway A, Ahlfors H, Turner M. The RNA-Binding Proteins Zfp36l1 and Zfp36l2 Enforce the Thymic beta-Selection Checkpoint by Limiting DNA Damage Response Signaling and Cell Cycle Progression. J Immunol. 2016; 197:2673–2685. [PubMed: 27566829]
31. Oliver AM, Martin F, Gartland GL, Carter RH, Kearney JF. Marginal zone B cells exhibit unique activation, proliferative and immunoglobulin secretory responses. European journal of immunology. 1997; 27:2366–2374. [PubMed: 9341782]
32. Leadbetter EA, et al. NK T cells provide lipid antigen-specific cognate help for B cells. Proceedings of the National Academy of Sciences of the United States of America. 2008; 105:8339–8344. [PubMed: 18550809]
33. Grajales-Reyes GE, et al. Batf3 maintains autoactivation of Irf8 for commitment of a CD8alpha(+) conventional DC clonogenic progenitor. Nature immunology. 2015; 16:708–717. [PubMed: 26054719]
34. Winkelmann R, Sandrock L, Kirberg J, Jack HM, Schuh W. KLF2--a negative regulator of pre-B cell clonal expansion and B cell activation. PLoS One. 2014; 9:e97953. [PubMed: 24874925]
35. Yeo JC, et al. Klf2 Is an Essential Factor that Sustains Ground State Pluripotency. Cell Stem Cell. 2014; 14:864–872. [PubMed: 24905170]
36. Revilla IDR, et al. The B-cell identity factor Pax5 regulates distinct transcriptional programmes in early and late B lymphopoiesis. The EMBO journal. 2012; 31:3130–3146. [PubMed: 22669466]
37. Keene JD. RNA regulons: coordination of post-transcriptional events. Nature reviews. Genetics. 2007; 8:533–543.

38. Kaymak E, Ryder SP. RNA recognition by the Caenorhabditis elegans oocyte maturation determinant OMA-1. The Journal of biological chemistry. 2013; 288:30463–30472. [PubMed: 24014033]
39. Farley BM, Ryder SP. POS-1 and GLD-1 repress glp-1 translation through a conserved binding-site cluster. Molecular biology of the cell. 2012; 23:4473–4483. [PubMed: 23034181]
40. Tamburino AM, Ryder SP, Walhout AJM. A Compendium of Caenorhabditis elegans RNA Binding Proteins Predicts Extensive Regulation at Multiple Levels. G3-Genes Genom Genet. 2013; 3:297–304.
41. Hoek KL, et al. Follicular B cell trafficking within the spleen actively restricts humoral immune responses. Immunity. 2010; 33:254–265. [PubMed: 20691614]
42. Santio NM, et al. Pim Kinases Promote Migration and Metastatic Growth of Prostate Cancer Xenografts. PLoS One. 2015; 10:e0130340. [PubMed: 26075720]
43. Grundler R, et al. Dissection of PIM serine/threonine kinases in FLT3-ITD-induced leukemogenesis reveals PIM1 as regulator of CXCL12-CXCR4-mediated homing and migration. J Exp Med. 2009; 206:1957–1970. [PubMed: 19687226]
44. Jain M, Zhang L, Patterson EE, Kebebew E. KIAA0101 is overexpressed, and promotes growth and invasion in adrenal cancer. PLoS One. 2011; 6:e26866. [PubMed: 22096502]
45. Aranda JF, et al. MYADM regulates Rac1 targeting to ordered membranes required for cell spreading and migration. Molecular biology of the cell. 2011; 22:1252–1262. [PubMed: 21325632]
46. Aranda JF, et al. MYADM controls endothelial barrier function through ERM-dependent regulation of ICAM-1 expression. Molecular biology of the cell. 2013; 24:483–494. [PubMed: 23264465]
47. Devis L, et al. Activated leukocyte cell adhesion molecule (ALCAM) is a marker of recurrence and promotes cell migration, invasion and metastasis in early stage endometrioid endometrial cancer. J Pathol. 2016
48. Nalvarte I, Damdimopoulos AE, Ruegg J, Spyrou G. The expression and activity of thioredoxin reductase 1 splice variants v1 and v2 regulate the expression of genes associated with differentiation and adhesion. Biosci Rep. 2015; 35
49. Hsiao SP, Chen SL. Myogenic regulatory factors regulate M-cadherin expression by targeting its proximal promoter elements. The Biochemical journal. 2010; 428:223–233. [PubMed: 20334626]
50. Reginato MJ, et al. Integrins and EGFR coordinately regulate the pro-apoptotic protein Bim to prevent anoikis. Nature cell biology. 2003; 5:733–740. [PubMed: 12844146]
51. de Boer J, et al. Transgenic mice with hematopoietic and lymphoid specific expression of Cre. European journal of immunology. 2003; 33:314–325. [PubMed: 12548562]
52. Hobeika E, et al. Testing gene function early in the B cell lineage in mb1-cre mice. Proceedings of the National Academy of Sciences of the United States of America. 2006; 103:13789–13794. [PubMed: 16940357]
53. de Luca C, et al. Complete rescue of obesity, diabetes, and infertility in db/db mice by neuron-specific LEPR-B transgenes. The Journal of clinical investigation. 2005; 115:3484–3493. [PubMed: 16284652]
54. Bouillet P, et al. Proapoptotic Bcl-2 relative Bim required for certain apoptotic responses, leukocyte homeostasis, and to preclude autoimmunity. Science. 1999; 286:1735–1738. [PubMed: 10576740]
55. Kim D, et al. TopHat2: accurate alignment of transcriptomes in the presence of insertions, deletions and gene fusions. Genome biology. 2013; 14:R36. [PubMed: 23618408]
56. Anders S, Pyl PT, Huber W. HTSeq--a Python framework to work with high-throughput sequencing data. Bioinformatics. 2015; 31:166–169. [PubMed: 25260700]
57. Love MI, Huber W, Anders S. Moderated estimation of fold change and dispersion for RNA-seq data with DESeq2. Genome biology. 2014; 15:550. [PubMed: 25516281]
58. Robinson JT, et al. Integrative genomics viewer. Nature biotechnology. 2011; 29:24–26.
59. Thorvaldsdottir H, Robinson JT, Mesirov JP. Integrative Genomics Viewer (IGV): high-performance genomics data visualization and exploration. Brief Bioinform. 2013; 14:178–192. [PubMed: 22517427]

60. Chen J, Bardes EE, Aronow BJ, Jegga AG. ToppGene Suite for gene list enrichment analysis and candidate gene prioritization. Nucleic acids research. 2009; 37:W305–311. [PubMed: 19465376]
61. Supek F, Bosnjak M, Skunca N, Smuc T. REVIGO summarizes and visualizes long lists of gene ontology terms. PLoS One. 2011; 6:e21800. [PubMed: 21789182]
62. Gautier L, Cope L, Bolstad BM, Irizarry RA. affy--analysis of Affymetrix GeneChip data at the probe level. Bioinformatics. 2004; 20:307–315. [PubMed: 14960456]
63. Langmead B, Trapnell C, Pop M, Salzberg SL. Ultrafast and memory-efficient alignment of short DNA sequences to the human genome. Genome biology. 2009; 10:R25. [PubMed: 19261174]
64. Zhang Y, et al. Model-based analysis of ChIP-Seq (MACS). Genome biology. 2008; 9:R137. [PubMed: 18798982]

Europe PMC Funders Author Manuscripts

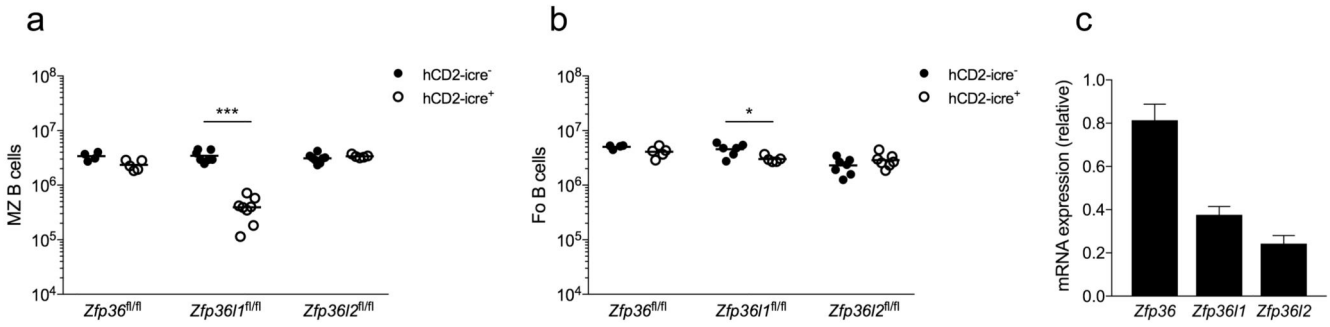

Figure 1.

Europe PMC Funders Author Manuscripts

Europe PMC Funders Author Manuscripts

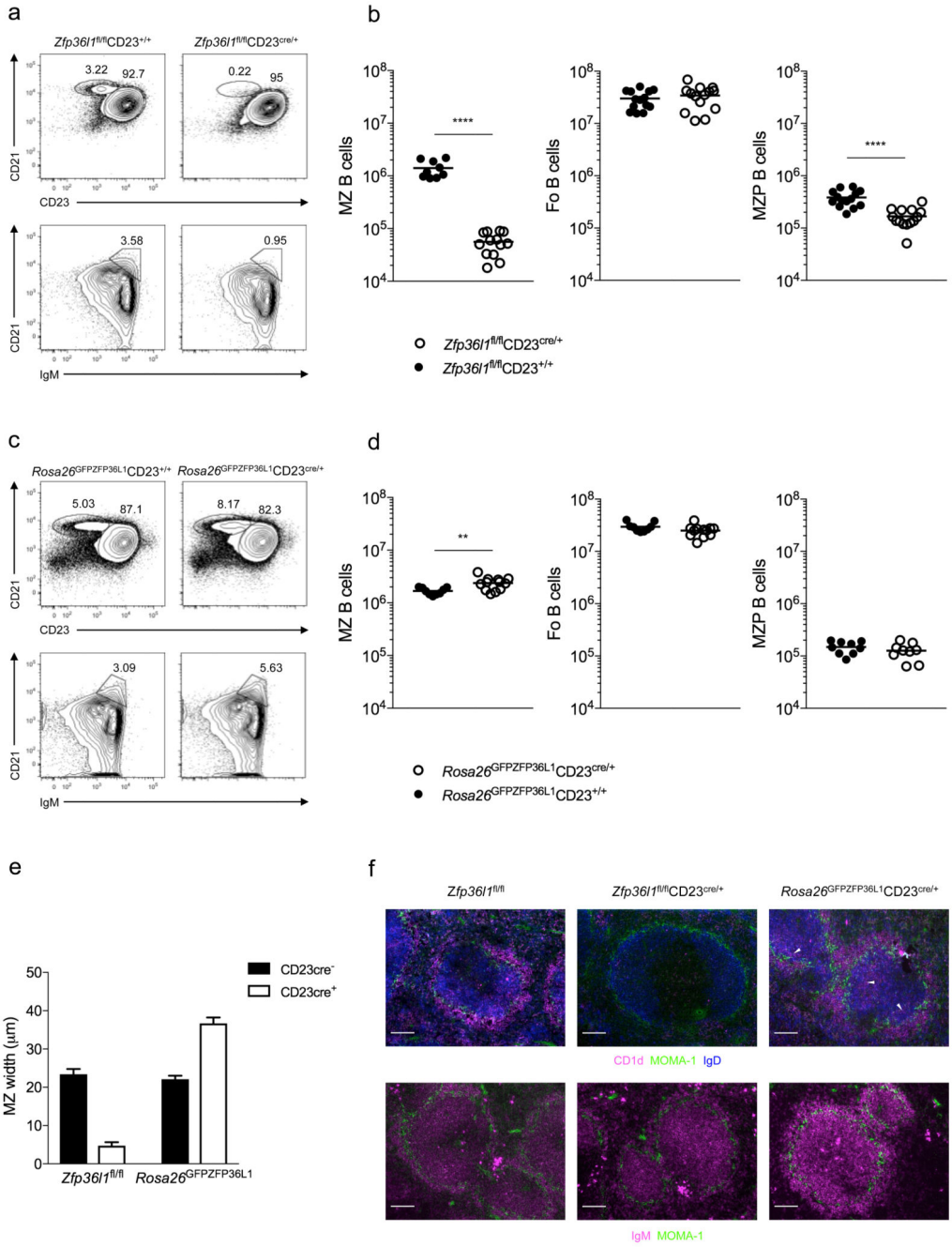

Figure 2.

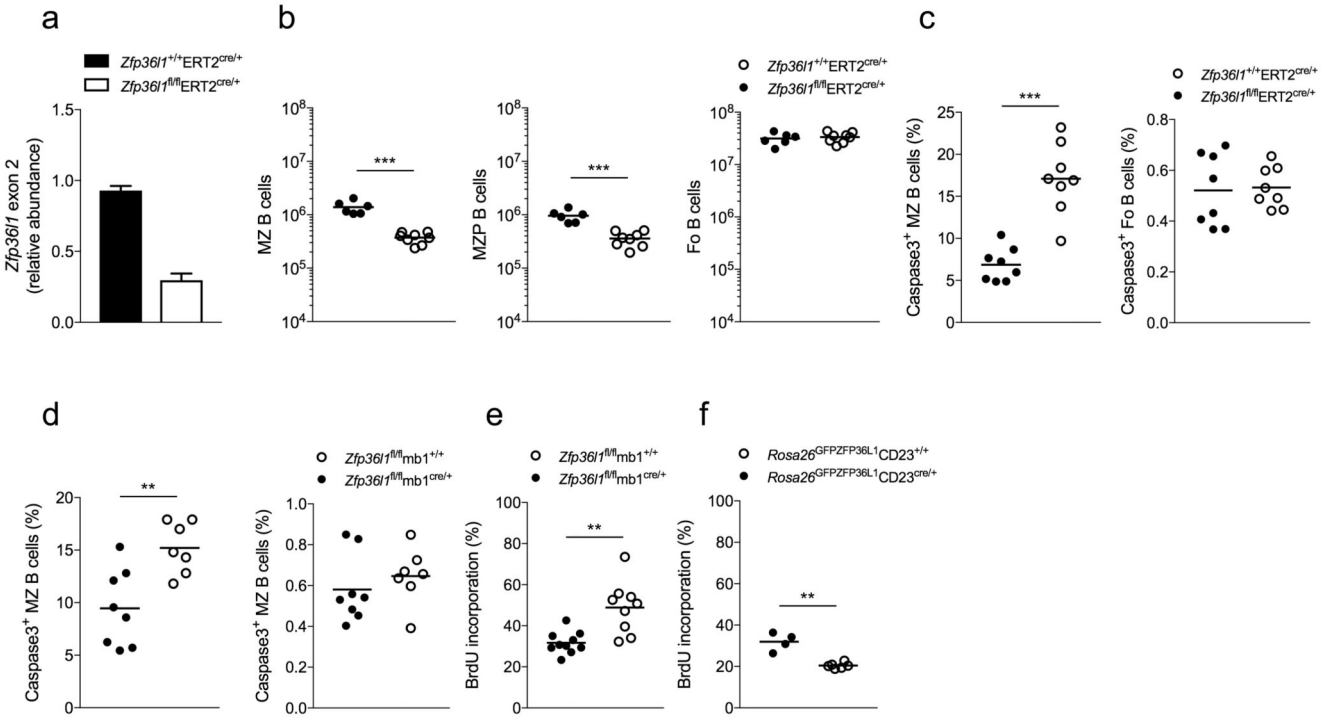

Figure 3.

Europe PMC Funders Author Manuscripts

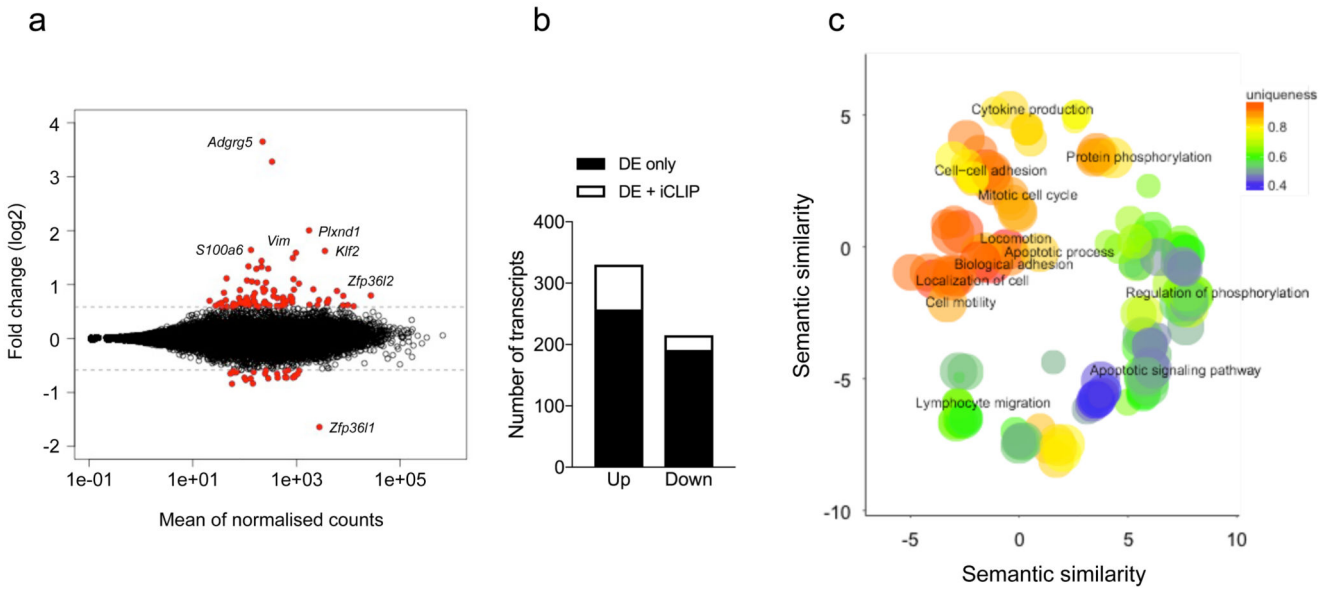

Figure 4.

Europe PMC Funders Author Manuscripts

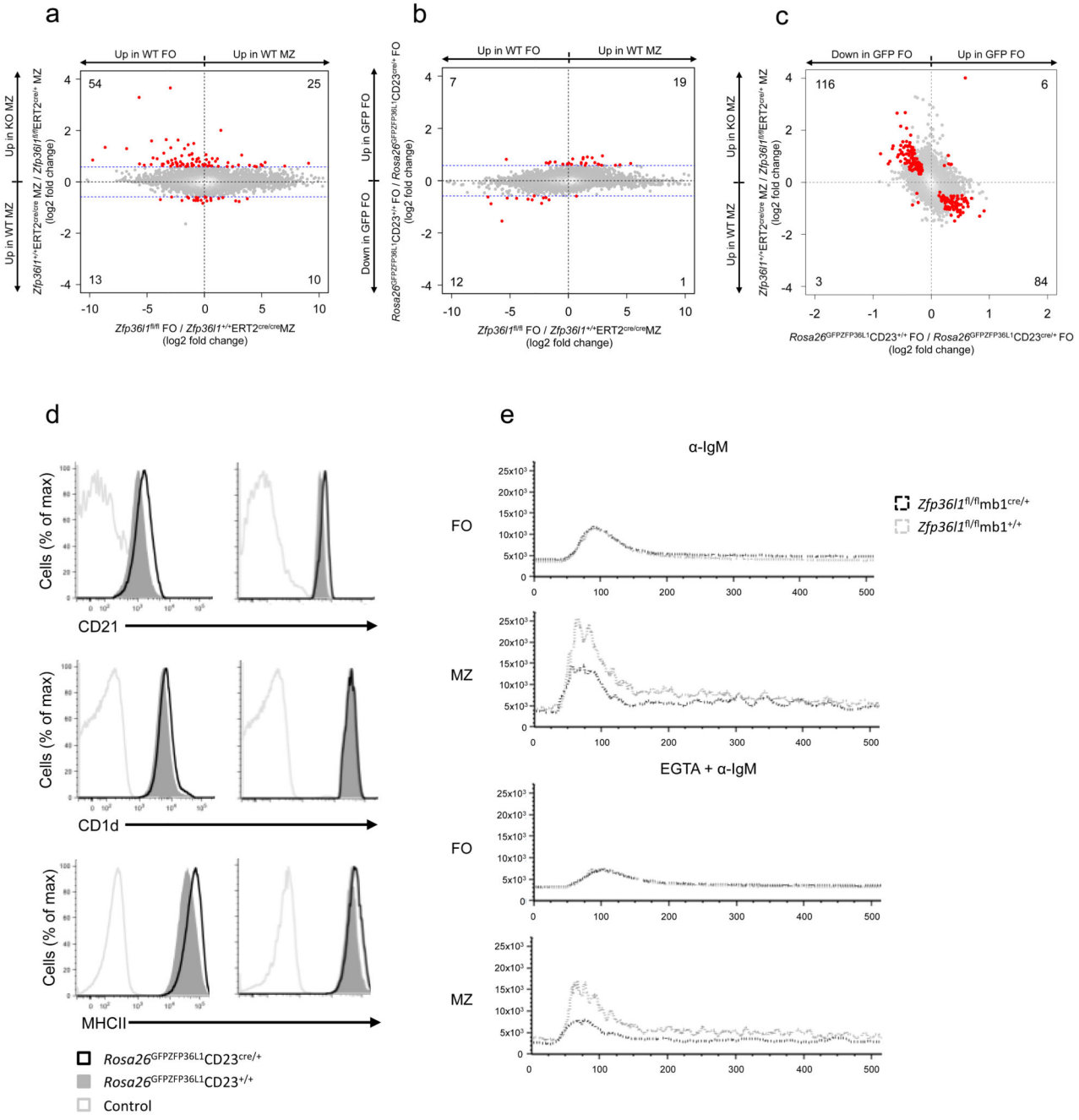

Figure 5.

Europe PMC Funders Author Manuscripts

Europe PMC Funders Author Manuscripts

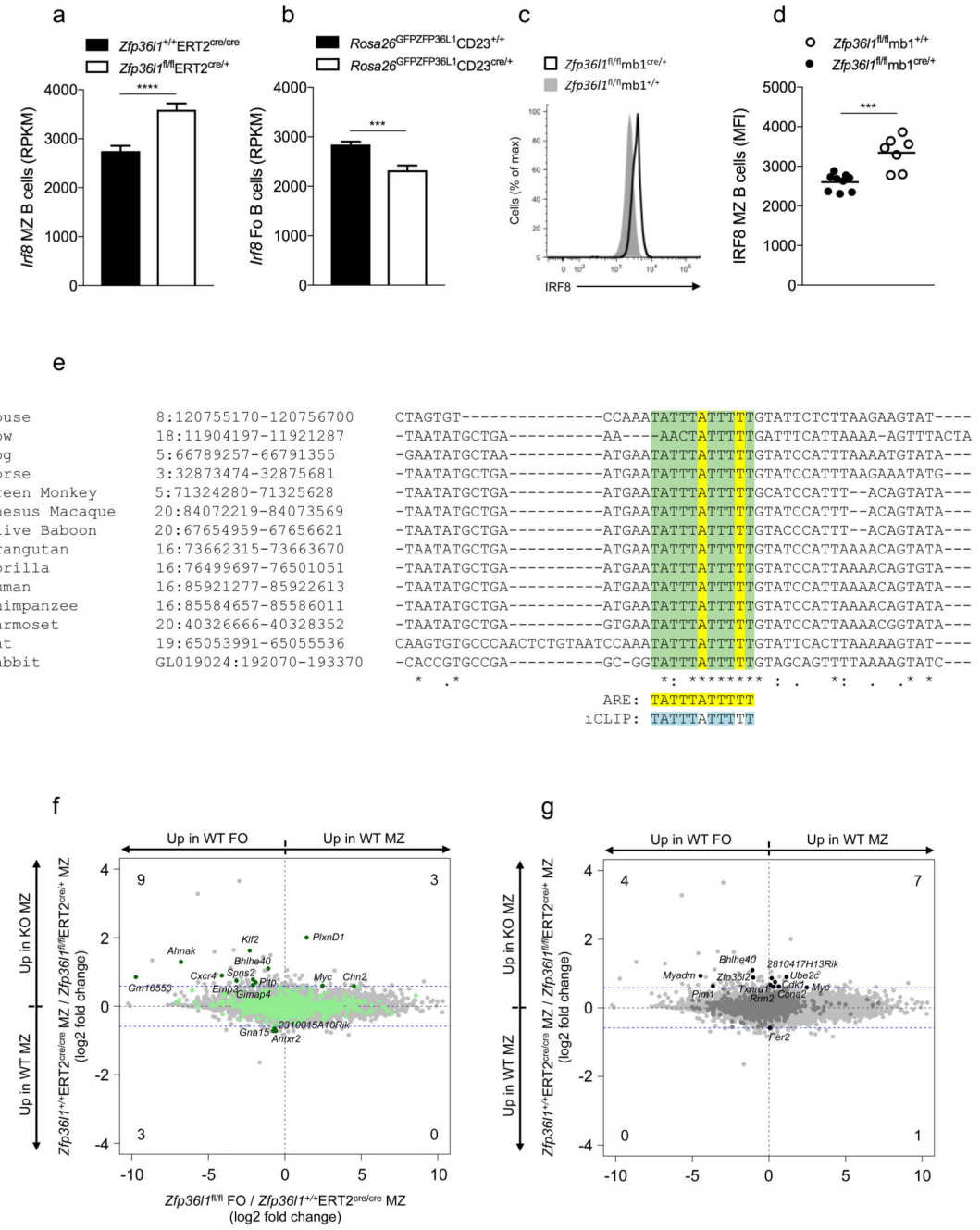

Figure 6.

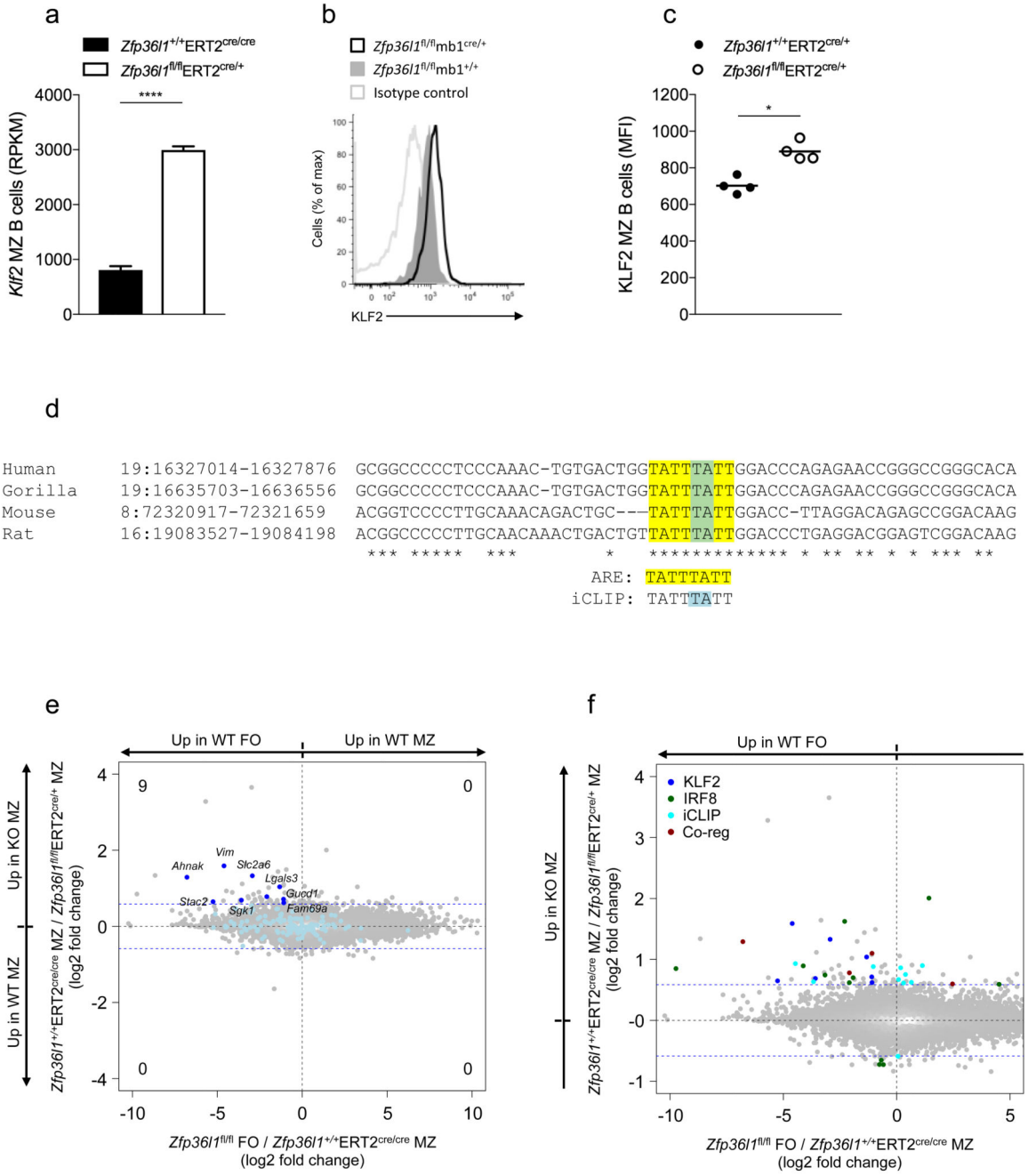

Figure 7.

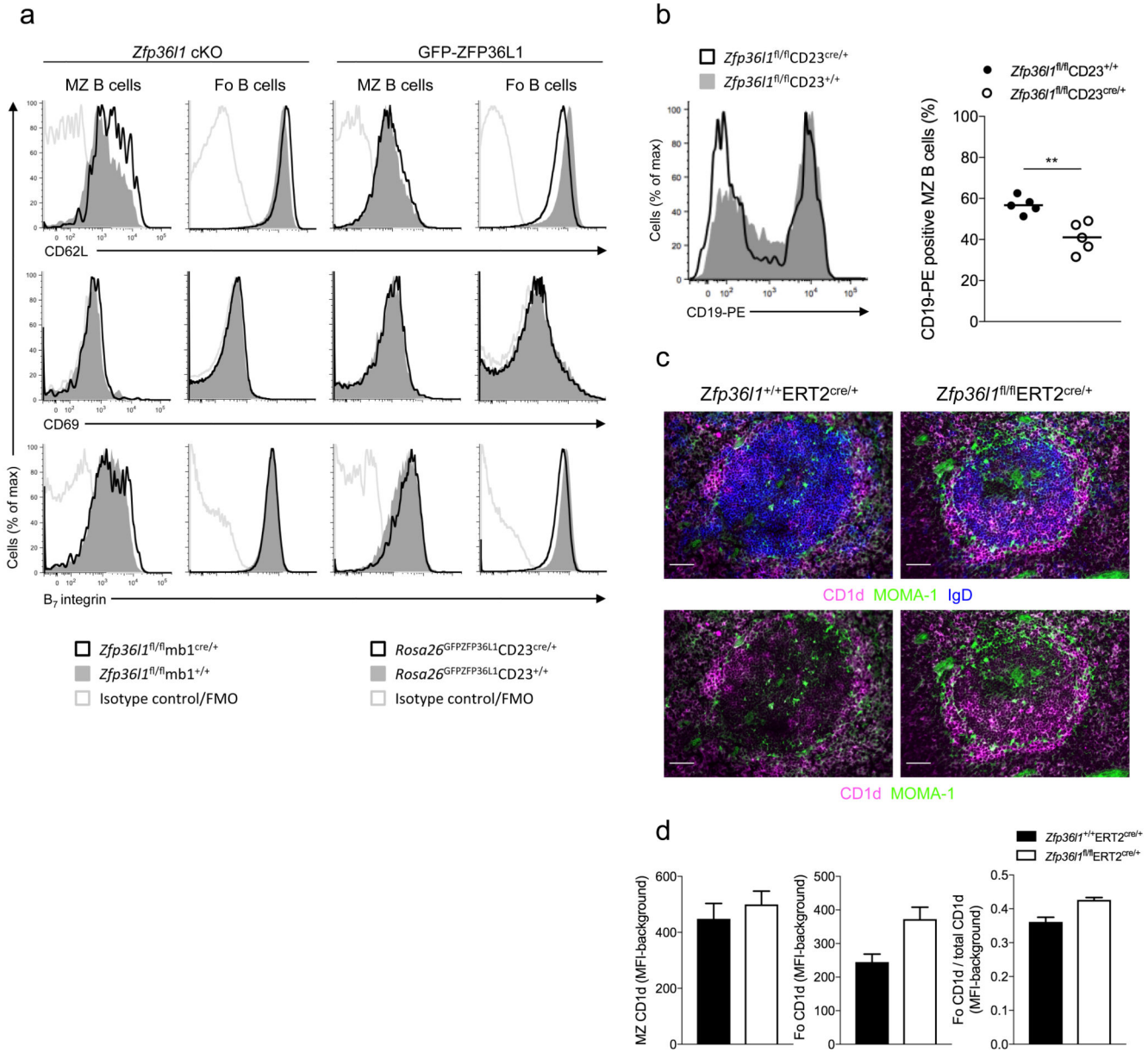

Figure 8.